JOURNAL OF CATALYSIS **163,** 186–194 (1996)
ARTICLE NO. 0318

Iron-Based Dehydrogenation Catalysts Supported on Zirconia

I. Preparation and Characterization

L. A. Boot,*,[1] A. J. van Dillen,* J. W. Geus,* and F. R. van Buren†

*Department of Inorganic Chemistry, Debye Institute, Utrecht University, P.O. Box 80083, 3508 TB Utrecht, The Netherlands; and †Dow Benelux N.V., P.O. Box 48, 4530 AA Terneuzen, The Netherlands

Received August 15, 1995; revised June 7, 1996; accepted June 12, 1996

Zirconia-supported iron oxide catalysts were prepared by incipient wetness impregnation, followed by drying and calcination in air. Characterization of the catalysts was performed with electron microscopy combined with element analysis (HR-TEM/EDAX), X-ray diffraction (XRD), temperature-programmed reduction (TPR), and thermomagnetic analysis. A homogeneous distribution of the iron containing phase can be obtained by using the metal complexes ammonium iron (III) citrate or ammonium (III) iron EDTA. A simple salt, such as iron nitrate, proved to be less suitable for this purpose. By HR-TEM/EDAX, it was shown that coverage of the zirconia support had been accomplished. XRD showed that crystalline Fe_2O_3 particles were formed at loadings $\geq$3 wt% Fe. TPR studies point to a bi-modal particle size distribution for the catalysts with 3 wt% Fe. Above this loading (>3 wt%) bulk properties prevail in TPR, whereas at lower loadings (<3 wt%) no distinct iron oxide species could be indicated. Magnetization measurements confirmed the results obtained by TPR. Catalysts prepared by coimpregnation of iron and potassium were also studied. TEM and XRD results show that a well-dispersed phase is obtained, but from XRD only potassium carbonate and no iron oxide or ferrite is evident. It was also found that the presence of potassium increases the onset of reduction of the iron phase by about 100°C.

1. INTRODUCTION

The use of a supported iron oxide catalyst can provide a successful remedy for overcoming the problems encountered with the industrially applied bulk catalysts used for the dehydrogenation of hydrocarbons, such as ethylbenzene (1, 2). The availability as commercial preshaped support bodies and proper physico-chemical properties (acid–base characteristics of the material, thermal, and chemical stability) are requirements for the support material. As discussed elsewhere (3), zirconia may be a promising support to be applied in dehydrogenation catalysts.

Since iron containing oxides are known to be favorable catalysts for dehydrogenation reactions (e.g., 4, 5), the development of a suitable preparation procedure for the present active phase-support combination is of interest. Therefore, the preparation, characterization, and catalytic testing of zirconia-supported iron-based catalysts were investigated. The preparation and characterization are reported in the present paper (part I).

Few examples of the iron-on-zirconia (powder) catalyst system are encountered in literature. This is due to the fact that zirconia has only recently been used and studied more often as a catalyst support material. When zirconia is used as a support in investigations on iron containing catalysts, it is usually incorporated in a series of various support materials. For example, Ji *et al.* (6, 7) performed a study on supported iron oxide catalysts, in which they also included zirconia. Essentially, the catalysts were prepared by one procedure, viz., adsorption from (excess) aqueous iron salt solutions under various conditions. Van Ommen *et al.* (8) investigated the preparation of iron oxide-on-zirconia by adsorption of iron acetylacetonate from organic solvents (as a minor part of a study on supported catalysts). The main goal of their work was to investigate the adsorption procedure itself. The most recent report in literature on a zirconia-supported iron catalyst is a paper by Guglielminotti (9), but no special attention was paid to the preparation of the catalyst (wet impregnation with iron nitrate of a precipitated zirconia). Spectroscopic studies were carried out to investigate the interaction between zirconia and reduced iron oxides. It was found that zirconia has a stabilizing influence on iron (II) species: spreading of these species caused a decreased reducibility of iron (III) via iron (II) to metallic iron.

The presently operated dehydrogenation processes use a fixed catalyst bed, which calls for mechanically strong catalyst bodies of at least some millimeters in diameter. In order to avoid shaping operations, the use of preshaped zirconia support bodies is required. Therefore, the results of suitable preparation procedures, such as impregnation of the preshaped support bodies with solutions of

[1] Present address: Akzo Nobel Chemicals B.V., P.O. Box 37650, 1030 BE Amsterdam, The Netherlands. E-mail: Ludo.Boot@Akzo.NL.

0021-9517/96 $18.00

chelating compounds, are of interest. Descriptions of the successful impregnation of preshaped support bodies with a solution of precursor compounds of the active component can be found in literature. Meima reported on the use of chelated complexes, such as metal–EDTA (ethylenediaminetetraacetate), metal–citrate, and metal–formate (10, 11), which yielded homogeneous distributions of the active phase throughout the wide-pore α-alumina support bodies. Stobbe (4, 12) extended this procedure to the preparation of iron-based dehydrogenation catalysts supported on magnesia. Again, chelating agents provided the best results because of their stabilizing influence on iron toward hydroxylation (and subsequent imhomogeneous precipitation) by the strongly basic magnesia support.

Although chelating agents have proved to be useful iron precursor compounds, the employment of a simple salt might be profitable if this also would produce a well-distributed iron phase on the zirconia support. Therefore, the application of metal complexes (ammonium iron (III) citrate, ammonium iron (III) EDTA) as well as a simple salt (nitrate) on to various preshaped zirconias has been studied in the present paper (part I). Characterization of the catalysts with transmission electron microscopy and X-ray diffraction is described. As a measure of the interaction between the applied iron oxide phases and the support the reducibility of the iron containing phase has been studied. The reduction behavior can also yield information on the phases which are formed during the dehydrogenation of 1-butane. The results of the study of the present catalyst system using this catalytic test reaction will be reported in part II of this work (this issue).

2. METHODS

Catalyst Preparation

Catalysts were prepared by incipient wetness impregnation, using three different preshaped zirconia carriers (3): Two batches of Daiichi RSC-H zirconia (designated I and II (3, 13); 100% monoclinic, pellets ϕ 3 mm); Engelhard L6132 zirconia (mixture of 60% monoclinic and 40% tetragonal modifications, pellets ϕ 3 mm) to study the influence of a different crystal modification; Norton XZ 16052 (100% monoclinic, extrudates ϕ 3 mm) to study the use of a differently shaped support. All supports were treated at 850°C in air for 16 h to obtain a stable specific surface area of about 20 m^2/g and a pore volume of about 0.25, 0.17, and 0.22 ml/g, for the three supports, recpectively.

Ammonium Fe(III) citrate (Merck, 28% Fe), ammonium Fe(III) EDTA (prepared according to Stobbe *et al.* (12)), or iron (III) nitrate nonhydrate (Merck, p.A.) were used as precursor compounds; aqueous precursor solutions were added to evacuated support bodies to obtain a loading of $\leq$3 wt% Fe. Higher loadings were obtained by multiple impregnation, with intermediate drying and calcination steps. Using the EDTA solution, the maximum attainable loading in one step is about 1.5 wt% Fe.

Potassium containing samples (typically $\leq$3 wt% K) were prepared by coimpregnation with an ammonium Fe(III) citrate and potassium carbonate solution.

The impregnation liquid was allowed to enter the support pellets for about 1 h at static vacuum. In order to investigate the influence of the drying rate catalysts were dried at room temperature either rapidly in flowing air for 2 h or slowly in static air for 16 h.

Finally, calcination of the samples took place in flowing air, by the following procedure: 150°C for 2 h, 500°C for 2 h, 750°C for 16 h (ramp between stages, 5°C/min).

A physical mixture of pretreated zirconium dioxide and iron (III) oxide (3 wt% Fe) was prepared by manually grinding the oxides in a mortar. The iron oxide was prepared separately by calcining ammonium Fe(III) citrate (Merck, 28% Fe) in air at 750°C for 16 h.

Characterization Techniques

Transmission electron microscopy. For electron microscopic studies samples were prepared by applying a few droplets of a dispersion of a finely ground catalyst ultrasonically treated in ethanol onto a holey carbon film supported by a copper grid. High resolution measurements and energy-dispersive element analysis were performed in a Philips CM-20 transmission electron microscope (200 kV) equipped with a field-emission gun.

Determination of textural properties. The specific surface areas of the bare supports and the catalysts were determined by nitrogen physisorption at liquid nitrogen temperature according to the BET-method. A surface area of 0.162 nm^2 for the physically adsorbed N_2 molecule was used for calculation of the BET surface area. Measurements were carried out either by dynamic physisorption (Quantasorb apparatus, Quantachrome Corp.) or by static physisorption (ASAP 2400, Micromeritics); the latter technique also provides a pore distribution up to 100 nm and information on the microporosity of the samples (*t*-plot method). Fractured samples of a particle size of 0.50–0.85 mm were outgassed at 200°C for 2 h prior to the measurements.

Powder X-ray diffraction. Powder XRD was carried out in a Philips powder diffractometer mounted on a Philips PW1140 X-ray generator using Fe$K\alpha_{1,2}$ radiation (1.93735 Å).

Temperature-programmed reduction. Reduction experiments were performed in an atmospheric (plug-)flow reactor using a thermal conductivity detector to monitor the hydrogen consumption. Water produced in the reduction reaction was frozen out using CO_2 (s/g) cold trap. A fractured catalyst sample (0.50–0.85 mm) was reduced in a 50 ml/min 10 or 70% (v/v) H_2/Ar gas flow, while the

temperature was changed from RT to about 900°C at a linear heating rate of 5°C/min.

Thermo-magnetical analysis. High-field magnetic measurements to study the reduction behavior were performed using a modified Weiss extraction technique as described by Stobbe *et al.* (14). The apparatus allowed *in situ* magnetization measurements at a field strength of 7000 Oe of fractured catalyst samples during heating/cooling in helium or reduction in 10% H_2/Ar up to 525°C with a heating/cooling rate of 0.5°C/min.

3. RESULTS AND DISCUSSION

Catalyst Preparation

All impregnation liquid utilized were able to wet the catalyst support bodies homogeneously and completely during the impregnation step. It was established that on all supports redistribution of the precursor over the support pellets occurred *exclusively* during the drying step. The drying step is known to greatly influence the macroscopic distribution of an impregnated phase within the support bodies (15). The subsequent calcination step did not further affect the obtained distribution.

Impregnation with ammonium iron (III) citrate produced homogeneously loaded catalyst pellets at both drying rates (3, 16). When using other precursors, i.e., iron (III) nitrate and ammonium iron (III) EDTA, the following observations were made. The use of nitrate always resulted in an eggshell distribution. As an alternative procedure the addition of small amounts of a compound which increases the viscosity of the solution, such as, e.g., agarose or hydroxyethylcellulose (HEC), was tried. This *route* to the final catalyst was, however, not continued, since no better results were obtained than when using only the complexing agents. With supports impregnated with ammonium iron (III) EDTA solutions only slow drying resulted in homogeneous distributions. Besides this effect, an influence of the pH of the impregnating solution could be observed, which has also been reported for silica-supported catalysts (17). With zirconia best results were obtained with EDTA solutions just above the uncorrected pH after preparation of the complex (pH $\approx$ 5.5), viz., at pH 6 or 7. Increasing the pH of the solution to higher values did not improve the distribution, but resulted in eggshell distributions after drying.

The above-mentioned results apply to catalysts with a typical Fe loading of about 3 wt% (or 1.5 wt% with EDTA solutions). Higher loadings (e.g., 6 or 9 wt% Fe) were obtained by multiple impregnation steps. Essentially the same effects were important as with catalysts containing 3 wt% Fe: usually catalysts with a higher loading were prepared starting with the homogeneously impregnated 3 wt% catalysts. It was established that the final distribution of the iron phase was determined by the distribution established during the first stage of the preparation: when an inhomogeneous loaded support body was impregnated, no improvement of the distribution could be achieved.

It was possible to obtain catalysts containing both iron and potassium with a macroscopically homogeneous iron distribution throughout the various supports. Again, optimal results were obtained using a low drying rate. However, the influence of the drying rate was less pronounced than with catalysts containing iron precursors only. Possibly the formation of a complex in which the ammonium group is replaced by a potassium ion plays a role here. Little is known in literature about both the solid state and the solution chemistry of these complexes, especially at concentrations approaching saturation as in the solutions used here. The formation of gaseous ammonia and carbon dioxide can be observed when preparing the impregnating solution (indicating the proceeding substitution reaction). Although the precise function of the ammonium citrate complex is not known as yet, it is conceivable that this replacement may induce different physico-chemical properties (crystallization behavior, viscosity, surface tension or adsorption, etc.). One or both of these modified properties may account for the better results of coimpregnation (17, 18). On the other hand, the mere presence of a higher amount of dissolved precursors probably increases the viscosity, which could also improve the desired characteristics of the solution for obtaining a homogeneous distribution.

When inspecting the catalysts after calcination, it was immediately clear that a different, olive green colored, phase had been formed. Moreover, the color changed to light brown very rapidly upon exposure to atmospheric air. This indicates that in the presence of potassium the formation of a potassium ferrite phase takes place. When no potassium was present, the catalysts all showed the reddish light-brown color (the brightness depending on the loading) characteristic of iron (III) oxides.

Transmission Electron Microscopy

Transmission electron microscopy (TEM) was performed on calcined Daiichi (batch I) zirconia-supported iron oxide catalysts. Discrimination between support crystallites and small crystalline iron oxide particles on the surface, which both exhibit diffraction contrast, is quite difficult. Therefore, it is hard to determine whether the active phase has indeed been applied onto the support surface. Using scanning electron microscopy the applied iron oxide cannot be observed. At high magnifications, a decoration of the zirconia crystallites by very small particles ($\phi < 0.5$ nm (3)) appears to be visible. This may be the applied iron oxide phase, but this effect could also be caused by surface roughness of the zirconia crystallites. In order to study the nature of this decoration, element analysis using a field emission gun providing an extremely narrow and bright electron beam was performed. A high surface concentration of iron could be

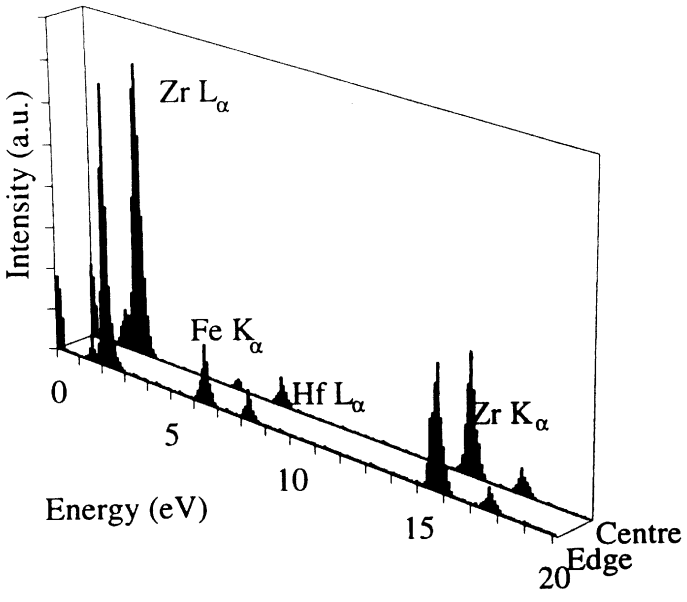

FIG. 1. Energy dispersive element analysis at the center and edge regions of a zirconia-supported catalyst crystallite (3 wt% Fe/ZrO_2).

detected when analyzing the edge of a support crystallite. When the surface of the zirconia crystallites is covered uniformly with small iron oxide entities, and we consider a zirconia platelet oriented perpendicularly to the electron beam, the thickness of the iron oxide layer in the direction of the electron beam is higher at the edge of the zirconia crystallite than at the center. Consequently, element analysis at the center leads to an iron-to-zirconium ratio that is lower than that measured at the edge. The results of this experiment are presented in Fig. 1 and Table 1. It can be derived that indeed a highly dispersed iron containing phase covering the zirconia surface is present.

In coimpregnated samples, the active components can be located more easily with TEM. It appeared that in samples in which 3 wt% iron and 3 wt% potassium had been deposited on zirconia the support is covered more or less completely with an apparently amorphous layer of deposited material (3, 16). Since these structures were completely absent in the bare support, it is supposed that the applied active components are present in this layer.

TABLE 1

Energy Dispersive Element Analysis Data for the Center and Edge Region of a Zirconia-Supported Catalyst Crystallite (cf. Fig. 1)

Location	Peak	At%	At% ratio
Edge	Zr$L\alpha$	49.57	1.0000
	Fe$K\alpha$	7.64	0.1542
	Zr$K\alpha$	42.75	0.8625
Center	Zr$L\alpha$	53.33	1.0000
	Fe$K\alpha$	0.93	0.0175
	Zr$K\alpha$	45.74	0.8577

TABLE 2

Textural Parameters of the Zirconia-Supported Catalysts

Catalyst	BET area (m^2/g)	S_μ (m^2/g)	Pore volume (cm^3/g)
ZrO_2	18.2	3.4	0.20
1 wt% Fe	18.0	3.3	0.19
3 wt% Fe	16.4	3.6	0.17
6 wt% Fe	11.2	2.4	0.14
9 wt % Fe	10.2	2.1	0.12
1.1 wt% Fe, K	16.0	3.0	0.18
3.3 wt% Fe, K	11.0	2.3	0.14
6.6 wt% Fe, K	7.3	1.3	0.10
9.9 wt% Fe, K	7.0	1.3	0.09

Note. S_μ denotes the micropore surface area determined according to the *t* method (3).

Catalyst Texture

The specific surface areas and pore structures of the catalysts with loadings up to 3 wt% Fe (Table 2) are similar to the textural parameters measured for the bare supports (3). When potassium is applied also, the pores are filled at lower iron loadings. The micropore surface follows the same trend. However, it is not reduced to zero at high loadings of iron and potassium.

X-ray Diffraction

The intense diffraction pattern of zirconia can obscure diffraction peaks originating from deposited active phases. Fortunately, the most intense diffraction peak of the ferric oxide expected to be formed after calcination of catalysts containing only supported iron oxide, viz. the peak due to the (104) plane of hematite (α-Fe_2O_3) at $d = 0.270$ nm, does not coincide with any of the zirconia peaks.

Diffractograms of the Fe/ZrO_2 catalysts (Fig. 2) show that a crystalline iron compound has been formed upon calcination at 750°C. In catalysts with homogeneous distributions of iron oxide, the most intense hematite diffraction peak (104) is hardly discernible from the noise in the diffractogram, indicating the presence of only a small amount of larger crystalline iron oxide particles. When a loading of less than 3% is applied, no hematite diffractions are detected.

When higher loadings (6 or 9 wt% Fe) are applied (Fig. 3), an increase of the intensity of the hematite (104) peak is observed. From the X-ray diffractograms it can be concluded that the additional amount of iron oxide deposited ends up largely in crystalline bulk iron oxide particles.

The particle diameters calculated from line broadening using the Scherrer equation (3) range from 20 to 30 nm for the 3 wt% Fe/ZrO_2 catalyst. No iron oxide particles of such dimensions were observed in TEM, but comparison

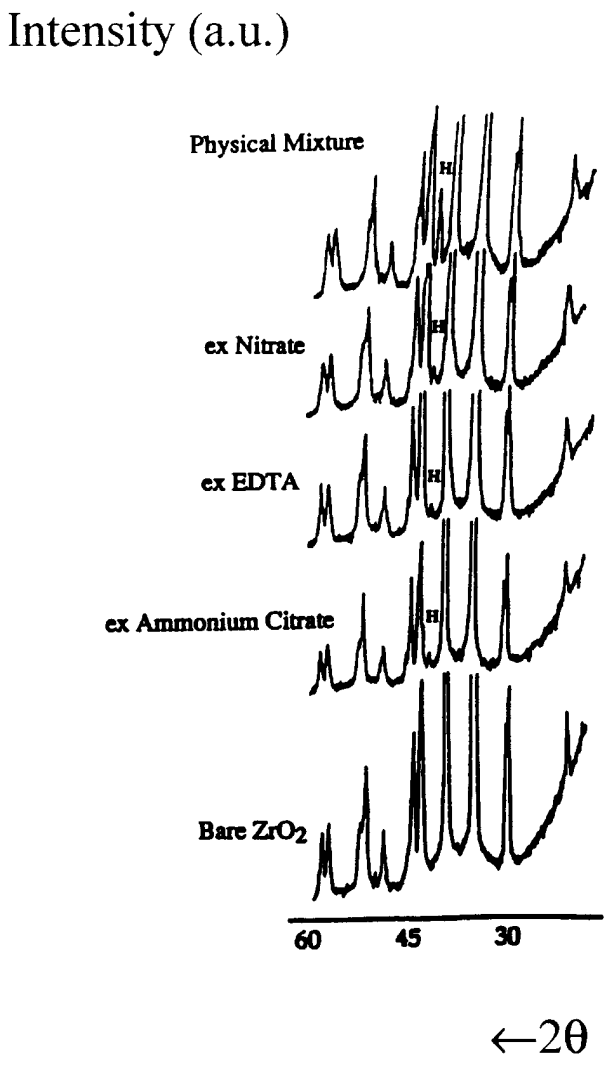

FIG. 2. X-ray diffractograms of 3 wt% Fe/ZrO_2 (Daiichi I) catalysts, prepared using various precursor compounds and of a physical mixture of iron oxide and zirconia (3 wt% Fe). H indicates the Fe_2O_3 (104) diffraction.

of the hematite peak intensities in the diffractograms of the 3 wt% Fe/ZrO_2 catalyst with that of a physical mixture with the same iron content (Fig. 2) suggests that only a small amount of these larger iron oxide crystallites was present. Moreover, the crystallinity of the support can obscure scarcely present hematite crystallites in TEM. The results therefore do not necessarily disagree.

XRD was also applied to the catalysts containing both iron and potassium. Since the olive green color of the zirconia-supported catalysts after calcination indicated the formation of potassium ferrite ($KFeO_2$), which is known to decompose readily in atmospheric air, diffractograms were recorded excluding air. These catalysts, although still olive green, exhibited only the lines of excess potassium carbonates (K_2CO_3 and $K_2CO_3 \cdot 3/2\ H_2O$), and no additional diffraction lines due to other phases than zirconia were detected (Fig. 4). Also after decomposition of potassium ferrite, characterized by the complete color change from olive green to brown, only potassium carbonate diffraction peaks were visible. These results are concordant with the TEM observations, which revealed the existence of an amorphous layer in the coimpregnated catalysts.

Temperature-Programmed Reduction

TPR profiles of zirconia-supported iron oxide catalysts are displayed in Figs. 5–9.

It was found that the application of two different hydrogen partial pressures, viz., 10 and 70% H_2 (v/v) in Ar, resulted only in trivial differences in the obtained reduction profiles (Fig. 5); i.e., the use of a higher hydrogen partial pressure caused the catalysts to be reduced completely at lower temperatures, while the use of a lower H_2 pressure gives a better resolution of the different reduction peaks. This can easily be explained by combining thermodynamic

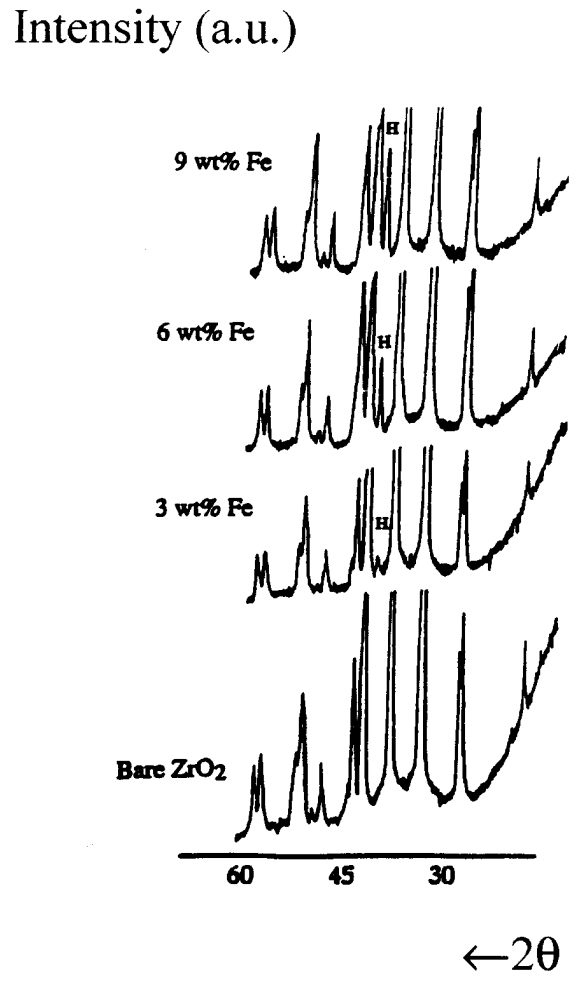

FIG. 3. X-ray diffractograms of 0, 3, 6, and 9 wt% Fe/ZrO_2 (Daiichi I) catalysts, prepared using ammonium iron (III) citrate. H indicates the Fe_2O_3 (104) diffraction.

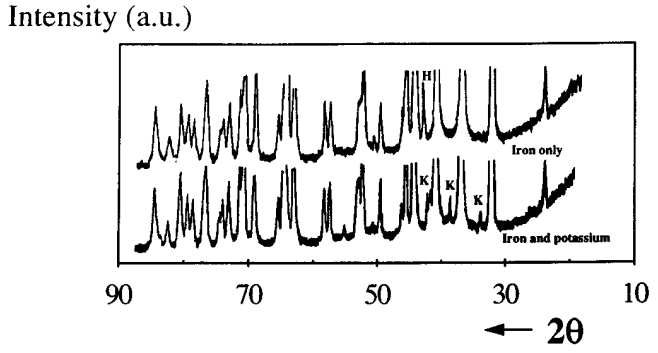

FIG. 4. X-ray diffractograms of 9 wt% Fe, 9 wt% K/ZrO_2, and 9 wt% Fe/ZrO_2 (Daiichi) catalysts, prepared using ammonium iron (III) citrate and potassium carbonate. H indicates the Fe_2O_3 (104) diffraction; K's indicate various potassium carbonate diffractions.

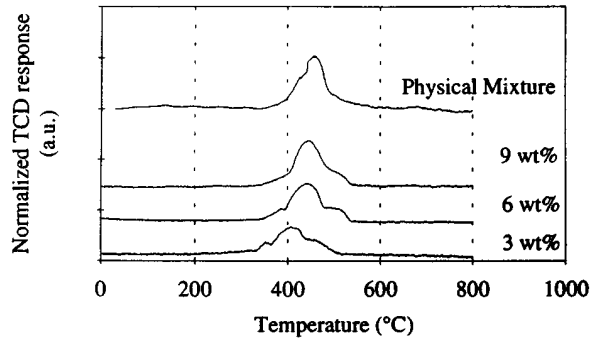

FIG. 6. Temperature-programmed reduction profiles (70% hydrogen in argon) of 3, 6, and 9 wt% Fe/ZrO_2 (Daiichi I) catalysts (ex ammonium iron (III) citrate) and of a physical mixture of iron oxide and zirconia containing 3 wt% Fe.

and kinetic effects: the higher pH_2/pH_2O ratio causes the reduction to complete at lower temperatures (19), and the higher H_2 concentration itself can increase the overlap of reduction peaks (20).

To attribute the reduction peaks to the transformations of distinct iron oxides by analyzing the reduction profiles only is difficult. In the (10% H_2) profiles of the catalyst ex citrate, e.g., at least four reduction stages can be seen (Fig. 5). It is obvious that the profile cannot be explained by stating that it represents the reduction of hematite via magnetite and wüstite to α-iron, as is done commonly (e.g., 8). It is more likely that a combination of effects is responsible for the complicated profiles. As was derived by combining the TEM and XRD results, both very small and larger iron oxide species are present in the catalysts. The difference in particle size itself can give rise to the occurrence of split peaks for essentially the same reduction reaction (21, 22) and also the difference in the stabilizing interaction that iron oxide species experience if they are either well-dispersed and in intimate contact with the zirconia support or more bulk-like and clustered together. The possible existence of such a stabilizing effect of oxidic supports on Fe^{2+} is well-documented in literature (e.g., 23, 24) and has recently been found to be operative in zirconia-supported iron oxide catalysts as well (9). Although the individual processes proceeding cannot easily be assigned, the TPR results can be used as a fingerprint for comparing the catalysts. It can be derived that the supported iron oxide phases experience an influence of the support which causes reduction of the iron phase to take place over a larger temperature range than is found with bulk catalysts and physical mixtures (8), suggesting the existence a certain degree of interaction with support.

When the loadings are increased, the reduction profiles resemble the profile displayed by the physical mixture; i.e., the reduction proceeds in a single unresolved step (Fig. 6). This is an agreement with XRD, which also revealed the presence of a more bulk-like iron oxide upon increasing the loading. When the loading is decreased (Fig. 7), the profile becomes less resolved, and less peaks exist. This seems to indicate the presence of less different types of iron oxide species in catalysts with loadings below 3 wt% Fe. From the normalized TPR profiles and the calculated final degree of

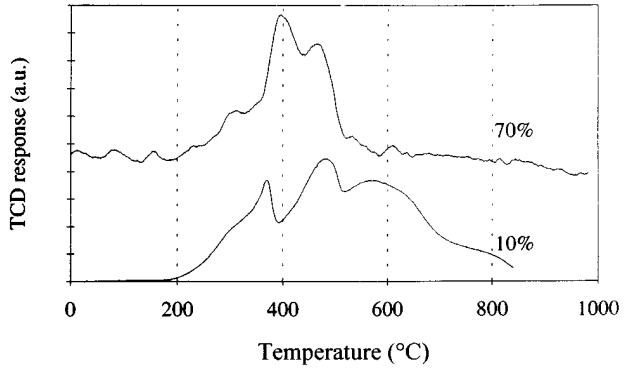

FIG. 5. Temperature-programmed reduction profiles of a 3 wt% Fe/ZrO_2 (Daiichi I) catalyst (ex ammonium iron (III) citrate) measured at different concentrations of hydrogen (10 and 70% in argon).

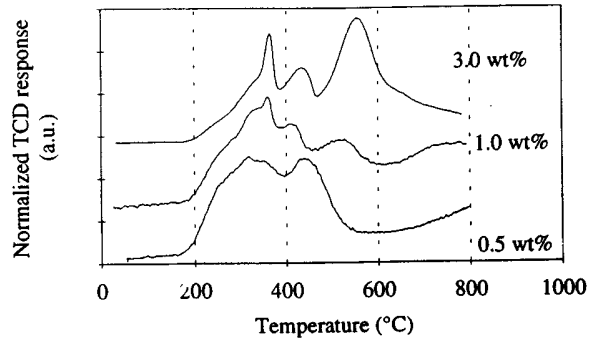

FIG. 7. Temperature-programmed reduction profiles (10% hydrogen in argon) of 0.5, 1, and 3 wt% Fe/ZrO_2 (Daiichi II) catalysts (ex ammonium iron (III) citrate).

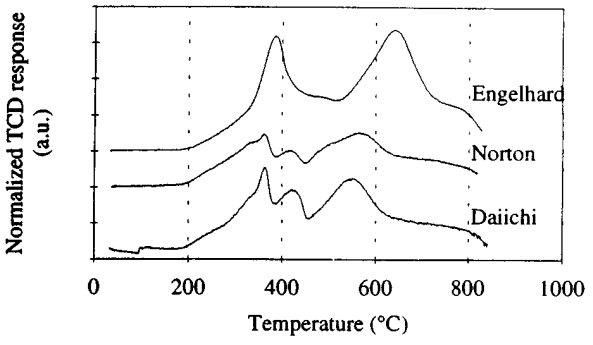

FIG. 8. Temperatrue-programmed reduction profiles (10% hydrogen in orgon) of 3 wt% Fe/ZrO_2 catalysts (ex ammonium iron (III) citrate) on various supports: Daiichi (II), Norton, Engelhard.

reduction (which approaches 100% with all catalysts), it can be concluded that reduction has completed at lower temperatures with the catalysts of the lowest loadings. This is likely to be caused by the smaller amount of water vapor to be removed from the pore system upon reduction of these catalysts.

Some more information can be derived about the interaction in catalysts prepared using different zirconia supports (Fig. 8) or different precursor compounds (Fig. 9). In catalysts containing only iron oxide as the active phase, it is observed that the first onset of reduction is at the same temperature with all samples. The samples supported on Norton ZrO_2 closely resemble the samples supported on Daiichi ZrO_2, whereas complete reduction is retarded in the catalysts prepared using the Engelhard support. An iron dispersion different from that mentioned above showing a few large iron oxide particles next to a large fraction of small iron oxide species has not been found for these catalysts with TEM nor XRD. The different reduction profile of the catalyst with the Engelhard zirconia must be attributed to other causes. As has been reported elsewhere (3), the large Engelhard support material displays a hydrogen consumption starting at about 600°C. The reduction of zirconia can therefore be expected to be observed in the reduction profile of the iron oxide supported on Engelhard. When the total hydrogen consumption is calculated for this catalyst, and the area of the second peak is subtracted, a value for the extent of reduction of iron oxide of around 100% results. In this catalyst, the reduction peaks of iron oxide and zirconia exhibit a considerable overlap, rendering any conclusions on the supported phase rather uncertain.

When comparing the catalysts ex EDTA and citrate supported on Daiichi (II) zirconia (Fig. 9), it is observed that in the case of EDTA a less resolved TPR profile is obtained. With the catalysts ex citrate of a lower loading (e.g., 1 wt% Fe) this was also observed. The lower loading of the catalyst ex EDTA (±1.4 wt% Fe) must be taken into account here: it seems that the same reduction behavior is observed for the catalyst prepared with either the citrate or the EDTA precursor.

Addition of potassium carbonate shifts the onset temperatures of the initial reduction to temperatures about 100°C higher than in catalysts without potassium (Fig. 10). This effect has been observed before (25). Possible explanations are the presence of a compound of iron and potassium (e.g., potassium ferrite) displaying a different reduction behavior; the coverage of the iron compound by potassium carbonate after decomposition of potassium ferrite limiting its accessibility for hydrogen; and the mere presence of the potassium compound, filling the catalyst pores and impeding the removal of water vapor. Whether the retarded reduction is caused by one or by a combination of more of the above-mentioned effects is difficult to assess.

Also effects of the particle size distribution, which have been mentioned when discussing the catalysts containing iron only apply here. Attribution of the separate peaks to discrete reduction processes will therefore not be feasible, with one exception. In agreement with Stobbe *et al.* (25), the reduction peak with an onset temperature of about 700°C is attributed to the reduction of potassium carbonate: the

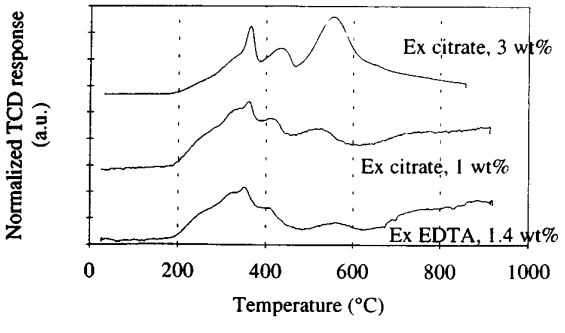

FIG. 9. Temperature-programmed reduction profiles (10% hydrogen in argon) of 1, 3, and 1.4 wt% Fe/ZrO_2 (Daiichi (II)) catalysts prepared using ammonium iron (III) citrate and ammonium iron (III) EDTA, respectively.

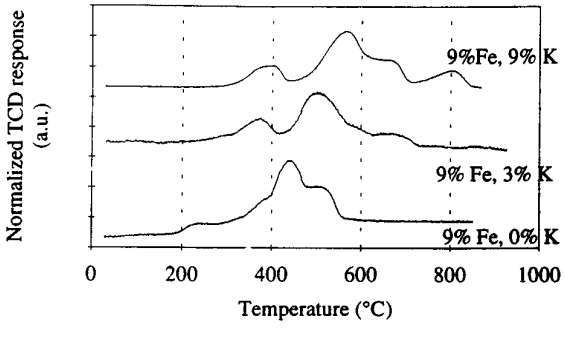

FIG. 10. Temperature-programmed reduction profiles (10% hydrogen in argon) of Fe, K/ZrO_2 (Daiichi) catalysts (ex ammonium iron (III) citrate and potassium carbonate). The reduction profile of a catalyst containing iron only is given as reference.

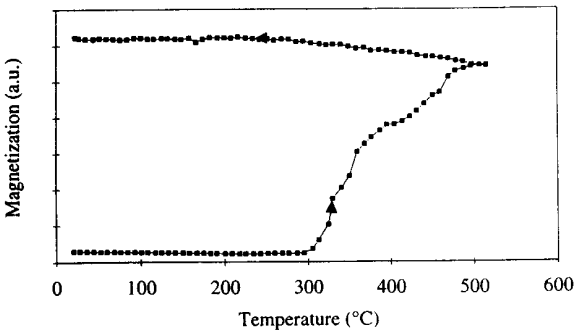

FIG. 11. Thermo-magnetic analysis profile (magnetization-versus-temperature) of a 3 wt% Fe/ZrO_2 (Daiichi I) catalyst (ex ammonium iron (III) citrate).

effect of the Fe/K ratio (Fig. 10) supports this attribution, since an increase of the potassium loading and therefore of the excess potassium carbonate content results in an increase in the height of this peak. Also *in situ* formation of potassium ferrite and simultaneous carbon dioxide evolution could be responsible for a positive detector signal, but this would require a substantial amount of remaining trivalent iron. The calculated total degree of reduction before the onset of the last peak (about 100%) excludes this possibility.

Thermo-magnetic Analysis

High-field measurements have been performed to follow the magnetic properties during TPR (Fig. 11). At the onset temperature of about 300°C formation of a magnetic phase, most probably magnetite, is observed. Then the magnetic signal shortly stabilizes, after which it increases, eventually to a high level, indicating the formation of magnetic iron. This is in agreement with TPR results in which the hydrogen consumption is measured, which also indicate a more or less parallel reduction of iron (III) and iron (II) taking place in the sample and show that predominantly Fe(0) is present at the end of the reduction experiments.

4. CONCLUSIONS

Procedures developed earlier for preparing supported iron catalysts by incipient wetness impregnation of preshaped support bodies can also be applied to zirconia supports. A homogeneous distribution of the iron containing phase can be obtained by using complex salts such as ammonium iron (III) citrate or ammonium iron EDTA. A simple salt such as iron nitrate proved to be less suitable. This confirms the results reported by other authors (4, 10–12, 17, 18). However, the effect of the pH with the EDTA precursor shows that valid results and hypotheses for one system (silica-supported iron oxide) cannot be generalized: the supposed effect of the tendency of the EDTA precursor to crystallize is either not operative here or is obscured by another parameter, e.g., the pore-size distribution. It was found that redistribution of the applied phases occurred only during the drying step.

By element analysis and HR-TEM, it was unambiguously demonstrated that a coverage of the zirconia support with very small iron oxide species had been accomplished. XRD showed that crystalline iron oxide particles were formed at loadings higher than 3 wt% Fe.

TPR experiments also point to bi-modal particle size distributions of the supported iron oxide, since complex reduction profiles are obtained at loadings of the active component higher than about 3 wt%. Above this critical loading bulk-like properties are displayed in TPR. At lower loadings (<3 wt% Fe) lower reduction temperatures are required for the complete reduction of the supported iron oxide. Magnetization measurements confirm the results obtained by TPR.

Catalysts prepared by coimpregnation with a solution of potassium iron (III) citrate which is obtained from ammonium iron (III) citrate and potassium carbonate were also studied. XRD results show that a well-dispersed supported phase results: only (excess) potassium carbonate and no iron oxide or ferrite is apparent. In combination with the fact that the olive green potassium ferrite formed initially decomposes very rapidly upon exposure to atmospheric air, all results support the conclusion that a well-dispersed supported active phase has been obtained. It was also found that potassium raises the temperature of the onset of reduction of the iron phase by about 100°C.

The performance of the presently prepared catalyst systems in the dehydrogenation of 1-butene, will be described in part II of this work (this issue). Zirconia is a suitable support for preparing a supported dehydrogenation catalyst: it disperses the iron oxide phase microscopically (TEM, XRD), it does not form bulk mixed compounds with iron or potassium (XRD), and the homogeneous application of the catalytically active phases throughout the catalyst support body is feasible.

ACKNOWLEDGMENTS

L. B. thanks M. W. J. van Soest, A. W. P. M. Strijbosch, W. J. Fok, H. J. Vermeer, and E. K. de Wit for experimental work and discussions and J. van de Loosdrecht for performing the TMA experiment. The HR-TEM/EDAX experiments were performed at the laboratories of Philips N.V., Eindhoven (the Netherlands).

REFERENCES

1. Herzog, B. D., and Rase, H. F., *Ind. Eng. Chem. Prod. Res. Dev.* **23**, 187 (1984).
2. Menon, P. G., *Chem. Rev.* **94**, 1021 (1994).
3. Boot, L. A., Ph.D. thesis, Utrecht University, 1994 (ISBN 90-393-0895-0).
4. Stobbe, D. E., Ph.D. thesis, Utrecht University, 1990.
5. Lee, E. H., *Catal. Rev.* **8**, 285 (1973).

6. Ji, W., Shen, S., Li, S., and Wang, H., *in* "Studies in Surface Science and Catalysis" (G. Poncelet, P. A. Jacobs, P. Grange, and B. Delmon, Eds.), Vol. 63, p. 517. Elsevier, Amsterdam, 1991.
7. Ji, W., Kuo, Y., Shen, S., Li, S., and Wang, H., *in* "New Frontiers in Catalysis" (L. Guczi, F. Solymosi, and P. Tétényi, Eds.), p. 2059. Elsevier, Amsterdam, 1992.
8. van Ommen, J. G., Bosch, H., Gellings, P. J., and Ross, J. R. H., *in* "Studies in Surface Science and Catalysis" (B. Delmon, P. Grange, P. A. Jacobs, and G. Poncelet, Eds.), Vol. 31, p. 151. Elsevier, Amsterdam, 1987.
9. Guglielminotti, E., *J. Phys. Chem*. **98**, 4884 (1994).
10. Meima, G. R., Ph.D. thesis, Utrecht University, 1987.
11. Meima, G. R., Dekker, B. G., van Dillen, A. J., Geus, J. W., Bongaarts, J. E., van Buren, F. R., Delcour, K., and Wigman, J. N., *in* "Studies in Surface Science and Catalysis" (B. Delmon, P. Grange, P. A. Jacobs, and G. Poncelet, Eds.), Vol. 31, p. 83. Elsevier, Amsterdam, 1987.
12. Stobbe, D. E., van Buren, F. R., Stobbe-Kreemers, A. W., Schokker, J. J., van Dillen, A. J., and Geus, J. W., *J. Chem. Soc. Faraday Trans.* **87**, 1623 (1991).
13. Boot, L. A., van Dillen, A. J., Geus, J. W., and van Buren, F. R., *J. Mater. Sci.*, in press.
14. Stobbe, D. E., van Buren, F. R., Hoogenraad, M. S., van Dillen, A. J., and Geus, J. W., *J. Chem. Soc. Faraday Trans.* **87**, 1639 (1991).
15. Knijff, L. M., Ph.D. thesis, Utrecht University, 1994 (ISBN 90-393-0328-2).
16. Boot, L. A., van Dillen, A. J., Geus, J. W., van Buren, F. R., and Bongaarts, J. E., *in* "Studies in Surface Science and Catalysis" (G. Poncelet, J. Martens, B. Delmon, P. A. Jacobs, and P. Grange, Eds.), Vol. 91. p. 159. Elsevier, Amsterdam, 1995.
17. van den Brink, P. J., Scholten, A., van Wageningen, A., Lamers, M. D. A., van Dillen, A. J., and Geus, J. W., *in* "Studies in Surface Science and Catalysis" (G. Poncelet, P. A. Jacobs, P. Grange, and B. Delmon, Eds.), Vol. 63, p. 527. Elsevier, Amsterdam, 1991.
18. van den Brink, P. J., Ph.D. thesis, Utrecht University, 1992 (ISBN 90-393-0153-0).
19. Wimmers, O. J., Arnoldy, P., and Moulijn, J. A., *Phys. Chem*. **90**, 1331 (1986).
20. Stuchly, V., *J. Therm. Anal.* **35**, 837 (1989).
21. Lemaitre, J. L., *in* "Characterization of Heterogeneous Catalysts" (F. Delannay, Ed.), p. 29, Dekker, New York, 1984.
22. Tonge, K. H., *Thermochim. Acta* **74**, 151 (1984).
23. Kock, A. J. H. M., and Geus, J. W., *Prog. Surf. Sci.* **20**, 165 (1985).
24. Wielers, A. F. H., Kock, A. J. H. M., Hop, C. E. C. A., Geus, J. W., and van der Kraan, A. M., *J. Catal.* **117**, 1 (1989).
25. Stobbe, D. E., van Buren, F. R., van Dillen, A. J., and Geus, J. W., *J. Catal.* **135**, 548 (1992).